Systematic kinetic analysis of mitotic dis- and reassembly of the nuclear pore in living cells

Elisa Dultz, Esther Zanin, Claudia Wurzenberger, Marion Braun, Gwénaël Rabut, Lucia Sironi, and Jan Ellenberg

Gene Expression Unit, European Molecular Biology Laboratory, D-69117 Heidelberg, Germany

During mitosis in higher eukaryotes, nuclear pore complexes (NPCs) disassemble in prophase and are rebuilt in anaphase and telophase. NPC formation is hypothesized to occur by the interaction of mitotically stable subcomplexes that form defined structural intermediates. To determine the sequence of events that lead to breakdown and reformation of functional NPCs during mitosis, we present here our quantitative assay based on confocal time-lapse microscopy of single dividing cells. We use this assay to systematically investigate the kinetics of dis- and reassembly for eight nucleoporin subcomplexes relative to nuclear transport in NRK cells, linking the assembly state of the NPC with its function. Our data establish that NPC assembly is an ordered stepwise process that leads to import function already in a partially assembled state. We furthermore find that nucleoporin dissociation does not occur in the reverse order from binding during assembly, which may indicate a distinct mechanism.

Introduction

Nuclear pore complexes (NPCs) mediate all traffic of macromolecules across the nuclear envelope (NE). They are large protein assemblies composed of multiple copies of ∼30 different proteins, the nucleoporins (Nups), which are organized in about 10 subcomplexes and arranged with eightfold symmetry. In metazoa, NPCs are stable throughout interphase (Daigle et al., 2001) but disassemble into their subcomplexes during mitosis. When the NE breaks down in pro/metaphase, most Nups become cytoplasmic and transmembrane Nups relocalize to the ER together with other nuclear membrane proteins (Ellenberg et al., 1997; Yang et al., 1997; Daigle et al., 2001; Beaudouin et al., 2002). Reassembly occurs during anaphase and telophase when the NE is rebuilt around chromatin.

In live cells, NE disassembly has been shown to start by partial disassembly of NPCs, with Nup98 leaving the NE early followed by dissociation of Nup153 and Nup214 before the NE is completely permeabilized. The membrane Nup POM121 dissociates from NE fragments only after permeabilization (Beaudouin et al., 2002; Lenart et al., 2003). In fixed cells, the nuclear basket Nup Tpr dissociates from the NE before Nup107 but later than Nup98 and Nup50 (Hase and Cordes, 2003).

More is known about the mechanism of postmitotic NPC assembly. In vitro studies of nuclear assembly in *Xenopus laevis* egg extracts have shed light on the essential role of the Ran–importin system, which regulates the release of several Nups from importin in proximity to chromatin, enabling them to reassociate and form NPCs (Harel et al., 2003a; Walther et al., 2003b). Several Nups bind to chromatin in early anaphase before membrane association (Belgareh et al., 2001; Walther et al., 2003a), where they have been postulated to form a prepore (Suntharalingam and Wente, 2003; Wozniak and Clarke, 2003; Rabut et al., 2004b). The mechanism of subsequent insertion into the membrane and full assembly of the NPC remains to be understood.

For some Nups, the order of reassociation with the reforming NE was investigated in various experimental systems, fixed cells of different mammalian species, or nuclei assembled in *X. laevis* egg extracts. Together, these data predict that the Nup107–160 complex, Nup153, Nup98, and POM121 bind during anaphase, followed by the Nup62 and Nup93 complexes, Nup358, and Nup214 in telophase, whereas Tpr and gp210 reassemble only in early G1 (for review see Burke and Ellenberg, 2002).

Evidence for structural disassembly and reassembly intermediates has been provided by field emission scanning electron microscopy. Porelike structures of different levels of complexity could be visualized in egg extract nuclei (Goldberg et al., 1997; Wiese et al., 1997; Kiseleva et al., 2001) and a rough time course of the formation of these structures could be established in *Drosophila melanogaster* embryos (Kiseleva et al., 2001). Their protein composition remained, however, unclear.

Our current knowledge predicts that NPC disassembly and reassembly are ordered processes that proceed via a defined set of intermediates formed by sequential interactions of NPC

E. Dultz, E. Zanin, and C. Wurzenberger contributed equally to this paper.

Correspondence to J. Ellenberg: jan.ellenberg@embl.de

Abbreviations used in this paper: IBB, importin β–binding domain of importin α; LBR, lamin B receptor; NE, nuclear envelope; NPC, nuclear pore complex; Nup, nucleoporin.

The online version of this paper contains supplemental material.

The Journal of Cell Biology, Vol. 180, No. 5, March 10, 2008 857–865
http://www.jcb.org/cgi/doi/10.1083/jcb.200707026

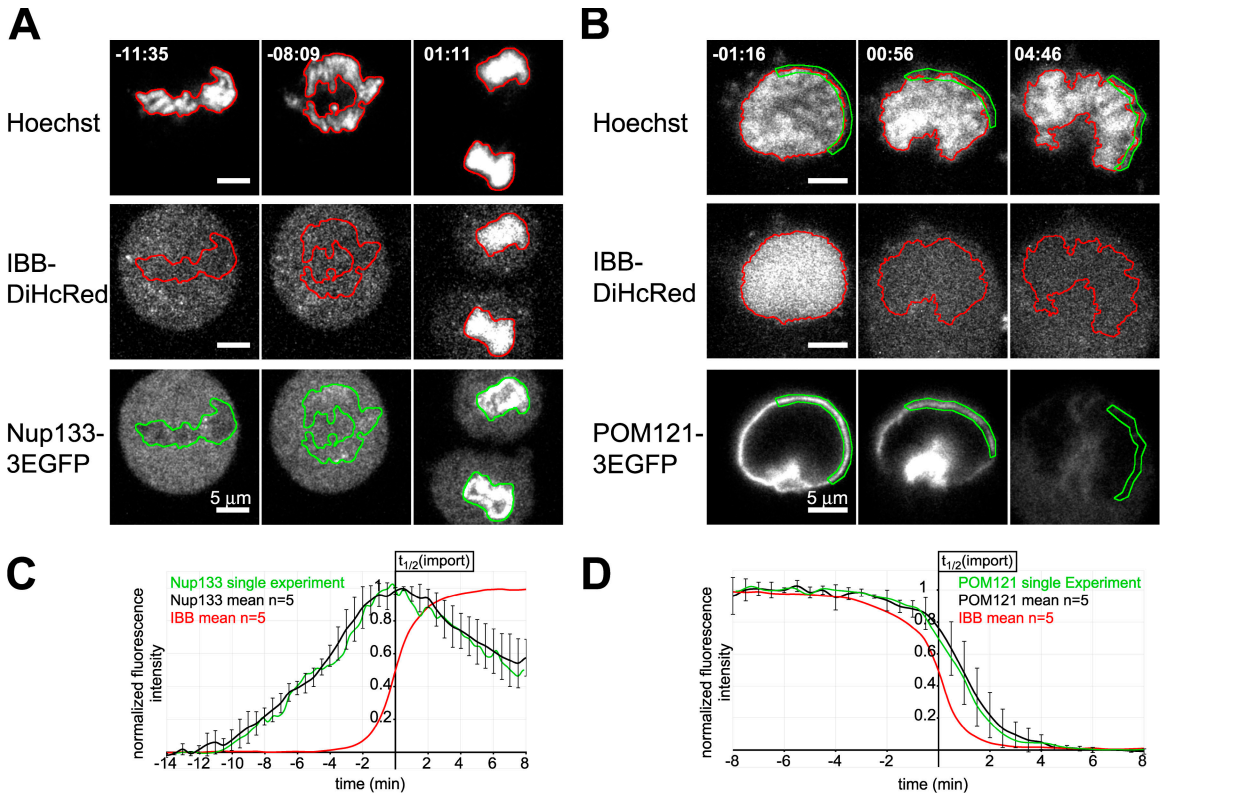

Figure 1. **Quantification of Nup and import marker fluorescence intensities.** (A and B) Regions of interest (outlines) were obtained from the Hoechst channel automatically (whole nucleus) or interactively (NE) and mean intensities were measured in the IBB and Nup channels. Time stamps give min:s relative to $t_{1/2}$(import). (C and D) Normalized Nup intensities over time extracted from sequences shown in A and B after alignment to $t_{1/2}$(import) (green). Black curves represent the mean of five independent experiments (error bars indicate SD). Red curves, IBB mean.

subcomplexes. However, the precise order in which the different subcomplexes bind, the kinetics of the assembly events, and the functional state of the different intermediates are unknown. To address this, we systematically investigated the kinetics of mitotic NPC disassembly and reassembly by time lapse confocal microscopy in single dividing cells. Simultaneously, we monitored import competence of the nucleus. We analyzed a set of GFP-tagged Nups (Rabut et al., 2004a) representing eight different NPC subcomplexes. Our results show that NPC assembly is indeed a highly ordered process that proceeds in a stepwise fashion. Partially assembled NPCs were already import competent, which indicates that several Nups may not be required to reestablish import function. Regarding NPC disassembly, we found it to occur more rapidly than assembly and not simply in the reverse order, which could indicate a distinct mechanism. Based on our data, we present the first comprehensive model for the order, composition, and functional state of NPC disassembly and reassembly intermediates in living cells.

Results and discussion

A functional and quantitative assay for the kinetics of NPC disassembly and reassembly

The kinetics of Nup dissociation from and reassociation with the NE during mitosis was monitored in live NRK cells expressing 11 GFP-tagged Nups representative of eight different subcomplexes (Rabut et al., 2004a): Nup133, Nup107, Seh1, and Nup43 (all from the Nup107–160 complex); the cytoplasmic Nup Nup214, Nup98, Nup58 (Nup62 complex), Nup93 (Nup93 complex); the nucleoplasmic Nups Nup50 and Nup153; and the transmembrane Nup POM121. In triple color time-lapse sequences of individual dividing cells, we recorded each GFP-Nup together with a red fluorescent nuclear import marker (importin β–binding domain of importin α [IBB]; Gorlich et al., 1996) and vital DNA staining (Fig. 1, A and B). DNA was used as spatial reference to quantify nuclear (envelope) intensities (for details see Materials and methods) and to monitor mitotic progression. The import marker IBB was efficiently imported into the nucleus during interphase, released into the cytoplasm at NEBD, and reimported in telophase, providing a functional reference for the import competence of the NPCs. In addition, we used the reimport/release of IBB to temporally align the assembly time series of the different Nups (Fig. 1, C and D). In summary, this assay allowed us to analyze the kinetics of NPC disassembly and reassembly in detail and to determine the import competence of the nucleus in different states of NPC assembly in living cells.

The Nup107–160 subcomplex binds to chromatin in early anaphase

Members of the Nup107–160 complex were the first to bind to chromatin in early anaphase. During mitosis, a small subpopulation of the complex localized to kinetochores as described

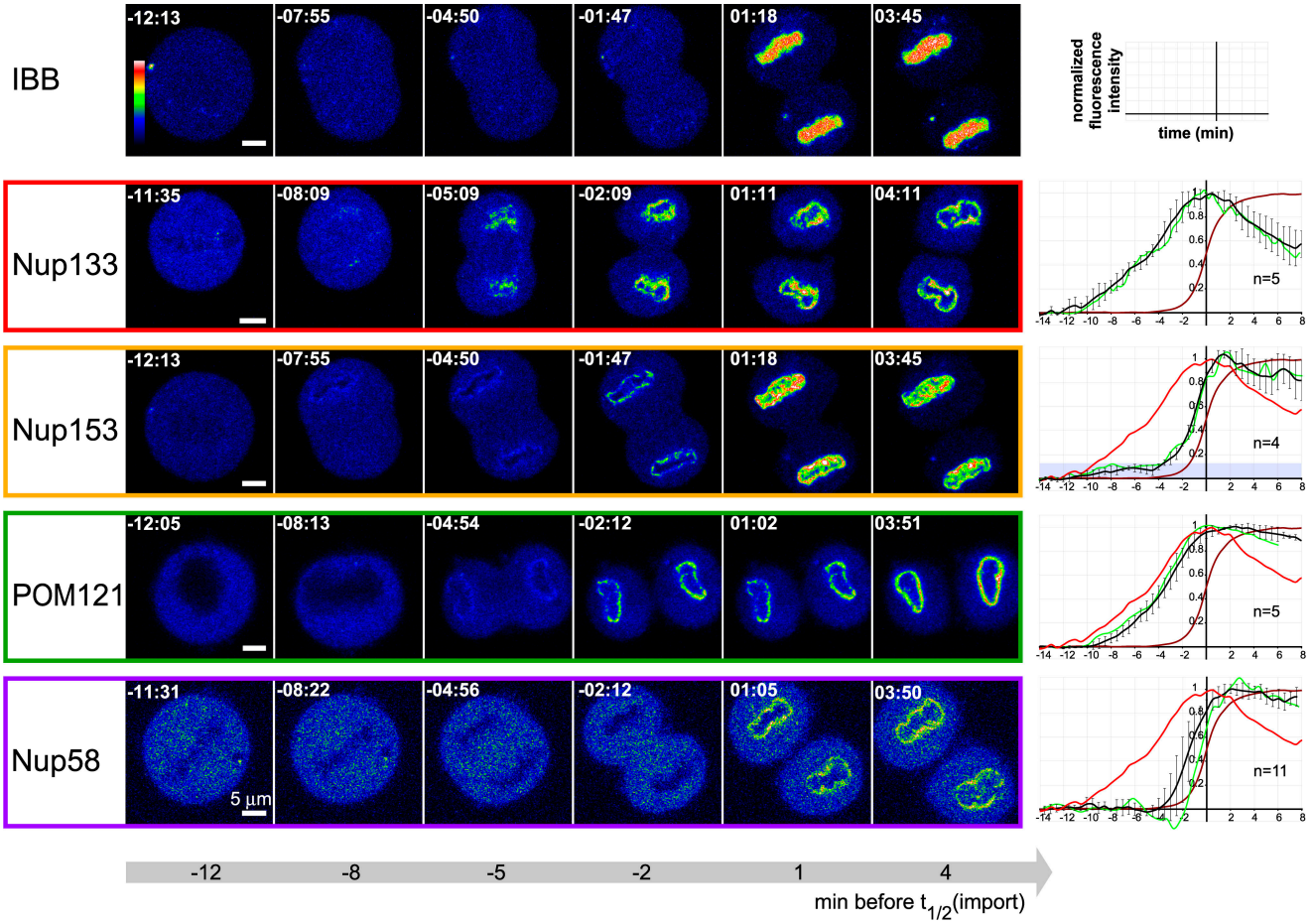

Figure 2. **Time series representing the assembly of four Nups.** The contrast of the image series was normalized to a common maximal mean intensity reached on the nuclear rim at the last time point of each series. Plots on the right show the data obtained from the series shown (green) and the mean of n series (black). As a reference, Nup133 (red) and IBB (dark red) intensity means are shown in all plots. Time stamps give min:s relative to $t_{1/2}$(import). Video 1 (available at http://www.jcb.org/cgi/content/full/jcb.200707026/DC1) shows representative full-image sequences for Nup133. Error bars indicate SD.

previously (Belgareh et al., 2001). General association of Nup133 with chromatin was detected shortly after the metaphase–anaphase transition or 8.5 ± 0.5 min ($n = 5$) before the time point of half maximal IBB intensity in the nucleus ($t_{1/2}$[import]; Figs. 2 and S1 A; and Video 1, available at http://www.jcb.org/cgi/content/full/jcb.200707026/DC1). Nup133 had already reached its maximal concentration at $t_{1/2}$(import). These observations are in line with the essential function of the Nup107–160 complex in NPC assembly observed in vitro (Boehmer et al., 2003; Harel et al., 2003b; Walther et al., 2003a; D'Angelo et al., 2006).

We analyzed the assembly of three additional proteins of this subcomplex (Nup107, Seh1, and Nup43). NPC subcomplexes are thought to be stable throughout the cell cycle (Matsuoka et al., 1999; Belgareh et al., 2001; Loiodice et al., 2004) and should thus bind to the reforming NE as a unit with identical kinetics. Indeed, we found Nup107 to faithfully recapitulate the assembly kinetics of Nup133 (Fig. S2 B, available at http://www.jcb.org/cgi/content/full/jcb.200707026/DC1). This suggests that stable subcomplexes are well represented by one member in our assay. Although the assembly of Seh1 and Nup43 also started early and was completed before $t_{1/2}$(import), their kinetics were slightly but consistently delayed relative to Nup107 and Nup133 during early anaphase. This could indicate that Seh1 and Nup43 are less stably associated with the complex and, indeed, this has been reported for Seh1 although not for Nup43 (Loiodice et al., 2004).

To test whether the binding of members of the Nup107–160 complex to chromatin represented formation of NPCs rather than a general "coating" of chromatin, we analyzed early assembly stages by high resolution microscopy of living cells. Binding of GFP-tagged members of the Nup107–160 complex to chromatin occurred in discrete patches and small dots of the appearance of single pores (Fig. 3 A). If these structures truly represent partially assembled NPCs, they should also contain Nups from other subcomplexes. We tested this by simultaneously imaging GFP-tagged Nup107–160 complex members and mCherry-tagged POM121. Indeed, POM121 first accumulated in patches around chromatin that also showed a strong localization of Nup107–160 complex members (Fig. 3 B). To rule out that this reflected the inability of the ER to contact other regions of chromatin in anaphase, we also analyzed the localization of mCherry-tagged lamin B receptor (LBR), a protein of the inner nuclear membrane known to bind to chromatin (Ye and Worman, 1994). In contrast to POM121, the localization of LBR was relatively smooth and did not show a bias for sites of Nup107–160 labeling (Fig. 3 C). Our data therefore suggest that Nup binding

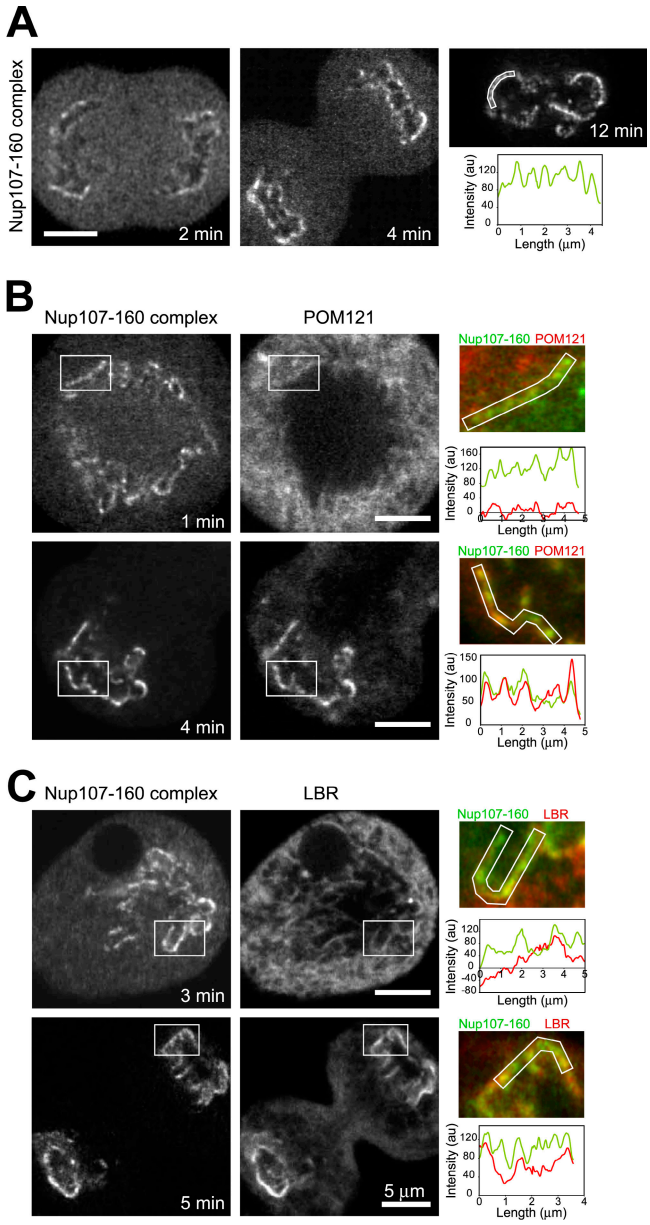

Figure 3. **Localization pattern of Nups on chromatin during anaphase.** Cells were followed from metaphase and single images were taken at defined time points. Images were filtered with an anisotropic diffusion filter. Boxes indicate regions of enlargements. Intensity profiles measured along a 0.45-µm-wide line as indicated by the white outlines were plotted after subtraction of cytoplasmic background. Time stamps indicate minutes after anaphase onset. (A) Cells expressing GFP-tagged Nup107, Nup133, and Nup37. (B) Cells expressing GFP-Nup107, GFP-Nup133, and POM121-mCherry. (C) Cells expressing GFP- Nup107, GFP-Nup133, and LBR-mCherry.

to chromatin in anaphase is caused by the formation of pore complexes and is consistent with the hypothesis that prepores form already on the naked chromatin before the attachment of nuclear membranes (Suntharalingam and Wente, 2003; Wozniak and Clarke, 2003; Rabut et al., 2004b).

Reassociation of Nup153 and Nup50 to the NE is biphasic

Nup153 and Nup50 localize to the nuclear basket and have been shown to exchange dynamically from the NPC with two residence times in interphase (Rabut et al., 2004a). In our assay, both Nup153 and Nup50 were detected at the periphery of the chromatin as early as 7.9 ± 1.4 (n = 4) and 6.6 ± 0.8 min (n = 6) before $t_{1/2}$(import), respectively (Figs. 2 and S2 A; and Video 2, available at http://www.jcb.org/cgi/content/full/jcb.200707026/DC1). However, this early pool accounted for <10% of the final nuclear intensity for Nup153 and only ∼20% for Nup50 (Figs. 2 and S2 A, blue shading). The major pools of these Nups associated with the NE considerably later and reached their half maximal intensity at the NE only 1.0 ± 0.3 (Nup153) or 1.1 ± 0.5 min (Nup50) before $t_{1/2}$(import) (see Fig. 5 D).

The biphasic assembly behavior we observed is consistent with the interphase dynamics and reinforces the interpretation that both proteins have two distinct modes of binding at the pore. Because both proteins are bound on the nucleoplasmic side of the pore, the early association of a small pool to chromatin could be involved in the formation of functional pores. The second phase of assembly paralleled initiation of nuclear import and transport through the first functional NPC assembly intermediates may therefore add the full complement of Nup50 and Nup153 to the complex.

POM121 accumulates at the NE after several soluble Nups

In interphase cells, the vertebrate-specific membrane Nup POM121 localizes almost exclusively to the NE, whereas it disperses in the ER during mitosis (Daigle et al., 2001). In metaphase, the ER is largely excluded from chromatin and spindle regions. However, ER membranes come close to the poleward face of the separating chromosomes early in anaphase (Fig. 3, B and C). The resulting early increase of POM121 signal around chromatin does therefore not reflect a specific accumulation (Fig. 3 B and not depicted). Accumulation in the NE over ER background became visible at 5.9 ± 1.0 min (n = 5) before $t_{1/2}$(import) and then rapidly reached its maximal intensity at $t_{1/2}$(import) (Fig. 2).

Together with the colocalization with the Nup107–160 complex, our kinetic data suggest that POM121-binding sites on chromatin become available only in late anaphase. At this time point, ER membranes come into physical contact with the separated chromosome masses from all sides and POM121 associates with chromatin at sites where Nup107–160 components are already bound.

Nup93, Nup98, and Nup58 assemble after membrane association

The Nup93 as well as the Nup62 complex are thought to localize to central positions of the pore. In our assay, the Nup93 and Nup62 complexes (represented by Nup58) accumulated at the NE starting at 3.8 ± 0.4 (n = 5) and 3.3 ± 1.4 min (n = 11) before $t_{1/2}$(import), respectively. The more peripheral Nup98 was first detected 3.8 ± 0.6 min (n = 6) before $t_{1/2}$(import) (Figs. 2 and S2 A). All three Nups reached their maximal intensity at the NE shortly after $t_{1/2}$(import).

Binding of these three complexes occurred only after several other Nups were already present on chromatin. Their addition may be the last step for the formation of an import competent NPC assembly intermediate because IBB import initiated concomitant

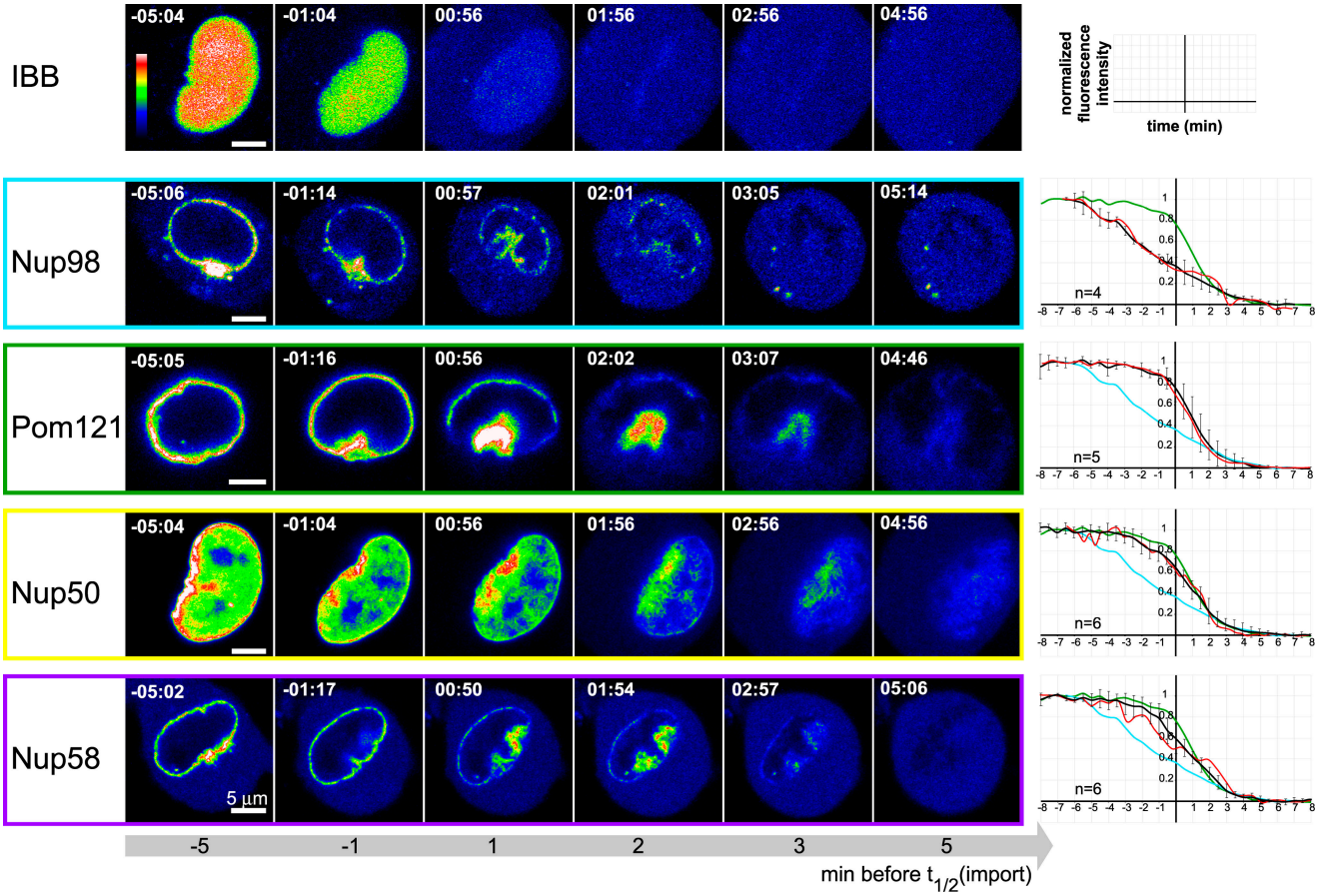

Figure 4. **Time series representing the dissociation of four Nups from the NE during prophase.** The contrast of the image series was normalized to a common maximal mean intensity on the nuclear rim at the first time point of each series. Plots show the data obtained from the series shown (red) and the mean of n series (black). As a reference, mean intensities of Nup98 (cyan) and POM121 (green) are shown in all plots. Time stamps give min:s relative to $t_{1/2}$(import). Videos 3 and 4 (available at http://www.jcb.org/cgi/content/full/jcb.200707026/DC1) show representative full-image sequences for Nup98 and POM121. Error bars indicate SD.

with their assembly (see Fig. 5, B and D). At this time, the Nup107–160 complex and POM121 were assembled already to ∼80%, whereas only the minor early fractions of Nup50 and Nup153 were present.

Nup214 association with the NE lasts well into G1

Nup214 is a peripheral cytoplasmic Nup with a residence time of several hours at interphase NPCs (Rabut et al., 2004a). We first detected Nup214 at the NE 0.8 ± 0.2 min ($n = 4$) before $t_{1/2}$(import) (Fig. S2). It was thus the last Nup to associate with the newly forming NPC investigated in this study. Its first appearance was concomitant with the regaining of nuclear import activity but its concentration continued to increase over cytoplasmic background long after the maximal IBB intensity in the nucleus was reached. High import rates were reached already when Nup214 had only reached 50% of its maximal intensity at the NE (see Fig. 5 D). These kinetics suggest that Nup214 may not be required for IBB import, which is consistent with previous findings that show no role of Nup214 in protein import via classical import routes but rather suggest an activity in protein export (Walther et al., 2002; Hutten and Kehlenbach, 2006). A newly assembled nucleus will likely have to establish import function first and export only later when nuclear biosynthesis has restarted. This would explain the late assembly time of factors not required for import such as Nup214.

NPC disassembly in prophase occurs rapidly and synchronously

The same set of eight representative Nups was followed during dissociation from the NE in prophase (Figs. 4, S1 B, and S3 A, available at http://www.jcb.org/cgi/content/full/jcb.200707026/DC1). Disassembly proceeded more rapidly than assembly and more synchronously for the different Nups so that distinct steps in the disassembly process could not be clearly resolved (compare Fig. 5, A and B). This could be caused by insufficient time resolution of the assay or simply the fact that disassembly occurs in fewer steps than assembly. Disintegration of a large part of the pore could be triggered in a single step. Also, recent EM data suggest that the disassembly of individual pores within one nucleus in *X. laevis* egg extract is asynchronous, leading to pore intermediates in different states of disassembly at the same time (Cotter et al., 2007). If this occurs in live mammalian cells, it would compromise our ability to detect the order of the process because we measure the mean of many pores simultaneously.

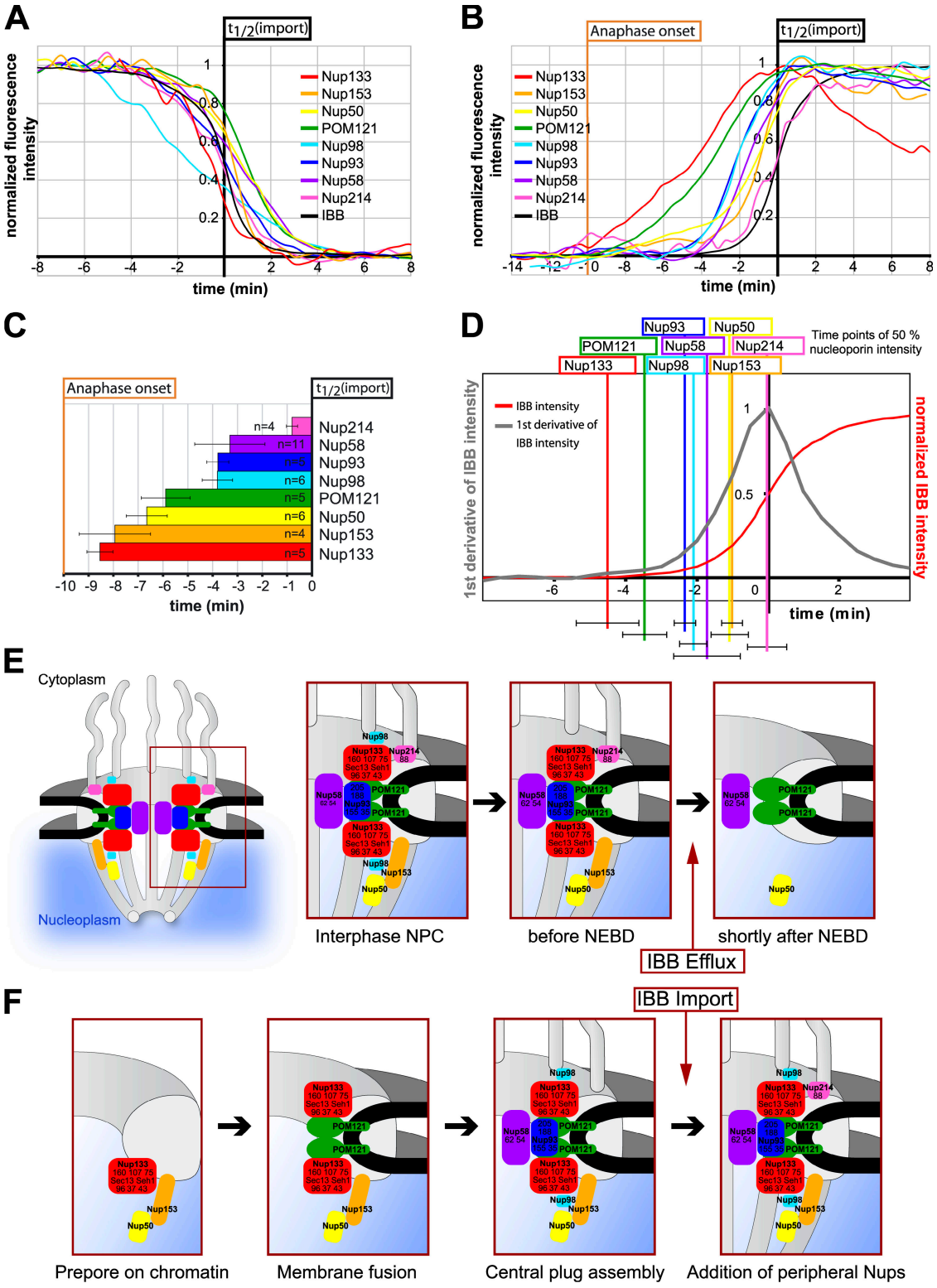

Figure 5. **Summary of NPC disassembly and reassembly kinetics.** (A and B) Overview over all means of disassembly (A) and assembly (B) kinetics. (C) Time points of first visible nuclear accumulation over background for all analyzed Nups. (D) Time points of 50% assembly of Nups relative to the first derivative of IBB intensity as a measure for import rate. Because of the change in concentration distribution of IBB between cytoplasm and nucleus during the import phase, the first derivative of IBB intensity systematically underestimates true instantaneous import rates. The maximum reached at time point 0 therefore does not reflect the true maximal import rates, which may be reached later. (E and F) Models for mitotic NPC disassembly and reassembly. Filament structures are included in the model in gray on the basis of previous data. The precise positions of the Nups in the NPC are unknown and thus drawn schematically. Because the different Nup-expressing cell lines showed some variability in the timing of mitotic progression (10.6 ± 1.5 min from anaphase onset to $t_{1/2}$[import]; not depicted), the time between anaphase onset and $t_{1/2}$(import) was normalized to 10 min in B to D. Error bars indicate SD.

Electron microscopy of *D. melanogaster* embryos has revealed disassembly intermediates similar to assembly; however, one intermediate dominated all prophase nuclei, indicating that other intermediates may be very transient (Kiseleva et al., 2001). This fits well with our observation in living mammalian cells that disassembly is very rapid. The similar ultrastructural appearance of NPC intermediates lead to the hypothesis that disassembly could be the reversal of assembly. Despite the limitations of our assay, our data indicate that this may not be the case. For example, the Nups that assembled earliest and latest during anaphase, i.e., Nup133 and Nup214, dissociated from the NE in the middle of the disassembly process. Nup98, which assembles at an intermediate time point in anaphase, was clearly the first Nup to dissociate from the nuclear periphery in prometaphase, which is in agreement with data from starfish oocytes (Lenart et al., 2003). Finally, Pom121, which is assembled after the Nup107–160 complex in anaphase, also dissociated clearly after the Nup107–160 complex during disassembly.

Interestingly, the Nup107–160, Nup93, and Nup214 complexes, which are the most stable NPC subcomplexes during interphase (Rabut et al., 2004a), dissociated early and rapidly, whereas Nup50 and Nup58 (Nup62 complex) together with POM121 remained longest in fragments of the NE (Figs. 4 and S3 A; and Videos 3 and 4, available at http://www.jcb.org/cgi/content/full/jcb.200707026/DC1). Thus, the NE identity of POM121-containing membranes appears to be lost only gradually in prometaphase, which is in agreement with previous observations (Beaudouin et al., 2002).

The persistence of Nup50 at the NE might be caused by chromatin rather than NPC association because we found Nup50 to coat chromatin throughout mitosis from prophase until anaphase (Fig. S3 B). It formed a dynamic coat, which rapidly exchanged with the cytoplasmic pool as assayed by photobleaching (unpublished data). This localization is consistent with the presence of the *Aspergillus nidulans* homologue of Nup50 on mitotic chromatin (Osmani et al., 2006) and could indicate a conserved mitotic function. However, it could also be caused by an inherent chromatin affinity of Nup50 because the yeast Nup50 homologue has been implicated in NPC associated gene regulation (Schmid et al., 2006).

Conclusion

In summary, our systematic study allows us to propose the first comprehensive model for mitotic NPC disassembly and reassembly (Fig. 5, E and F). Disassembly occurs in mammalian cells in a similar manner to starfish oocytes (Lenart et al., 2003) but with faster kinetics (Fig. 5 A). The composition of disassembly intermediates appears to differ from assembly intermediates, which suggests a distinct mechanism.

Our data provide detailed insight into the kinetics of pore assembly with high time resolution. Consistent with previous studies, we find NPC assembly to be a highly ordered process (Fig. 5 C). For the first time, we can relate the composition of the different assembly intermediates to import function. Our data supports the model that assembly starts with formation of a prepore on chromatin and indicates that such a structure contains the Nup107–160 complex as well as substoichiometric amounts of Nup153 and Nup50 (Fig. 5 F). These may provide the binding platform for additional components like the transmembrane Nup POM121.

In our live cell assay, we measure the mean concentration of Nups over all NPCs in the imaging plane to determine their assembly kinetics. We therefore cannot formally decide whether the fact that the association kinetics of individual Nups stretch over several minutes reflects asynchronous assembly of different NPCs in the nucleus, the sequential addition of multiple copies of the same Nup to NPCs in the same state of assembly, or a mixture of the two processes. However, our high-resolution imaging data showed similar concentration of Nups in adjacent pores at single time points during assembly (Fig. 3). Furthermore, electron microscopic data from *D. melanogaster* indicate that specific assembly intermediates dominate at any stage of mitosis (Kiseleva et al., 2001). We therefore assume that our kinetics reflect at least to a large extent the synchronous assembly process of many NPCs after mitosis.

What then is the first assembly intermediate that is competent for nuclear import? Comparing the time of half maximal concentration for each Nup with the rate of import (Fig. 5 D), our data show that the assembly intermediate containing mainly the Nup107–160 complex and POM121 does not support protein import (Fig. 5, B and D). Only upon association of Nup93, Nup58 (Nup62 complex), and Nup98 does IBB import initiate, which suggests that these complexes add transport activity to the new pore, possibly by providing many phenylalanine-glycine repeats. At this time point, at least a fraction of the pores in the nucleus contain all subunits necessary to support protein import function. In addition, the presence of a sealed or nearly sealed membrane around the nuclear compartment is likely required for IBB to accumulate in the nucleus. In contrast, the nucleoplasmic Nup50 and Nup153 as well as the cytoplasmic Nup214 are probably not required for import activity in stoichiometric amounts.

In the future, it will be very interesting to analyze the behavior of additional Nups, especially the membrane-bound Ndc1 and ELYS/Mel28, which have very recently been reported to play crucial roles in NPC assembly (Galy et al., 2006; Mansfeld et al., 2006; Rasala et al., 2006; Stavru et al., 2006; Franz et al., 2007). In addition, similar data obtained for interphase assembly will allow to test whether the insertion of NPCs into an intact interphase NE follows the same mechanism as postmitotic assembly.

Our assay using IBB as a functional and temporal marker should furthermore prove very useful to study additional aspects of NEBD and NE assembly. Besides a detailed kinetic understanding, the assay can also yield mechanistic insight when combined with molecular perturbations by RNAi or the expression of dominant-negative proteins.

Materials and methods

DNA constructs and cell lines

pIBB-DiHcRed was generated by ligating the fragment of the IBB domain from the plasmid pQE60-IBB-GFP (Ribbeck and Gorlich, 2002) into pDiHcRed-N1 (Gerlich et al., 2003) with a 5–amino acid linker (GPVAT) between the IBB domain and DiHcRed.

pPOM121-mCherry was cloned by exchanging 3EGFP in pPOM121-3EGFP (Rabut et al., 2004a) with mCherry (Shaner et al., 2004). pLBR1TM-mCherry contains the N terminus of LBR and its first transmembrane domain.

It was cloned by exchanging YFP in pLBR1TM-YPF (Daigle et al., 2001) with mCherry.

NRK cells were grown in standard medium. NRK cell lines stably expressing Nups tagged with EGFP (Nup50, Nup58, Nup93, Nup98, Nup133, Nup153, Nup214, Pom121, Nup43, and Seh1) as described previously (Rabut et al., 2004a) were maintained at 0.5 mg/ml G418. Some experiments were performed by transient transfection with the same plasmids used for generation of the stable cell lines. Transient transfections with pIBB-DiHcRed and Nup plasmids were performed with FuGene 6 (Roche) 24–72 h before imaging. For dual-color high-resolution imaging (Fig. 3), cells coexpressing GFP-tagged members of the Nup107–160 complex and LBR- or POM121-mCherry were enriched by FACS.

Live cell microscopy

For live cell microscopy, cells were grown in Lab-Tek chambered coverglasses (Thermo Fisher Scientific). 30 min before imaging, the medium was exchanged for prewarmed CO_2-independent medium without phenol red supplemented with 20% FCS, 2 mM glutamine, 100 mg/ml penicillin and streptomycin, and 0.2 µg/ml Hoechst 33342. The chambers were sealed with silicone grease. Time lapse sequences of 2–4-µm thick confocal slices were recorded at 37°C on confocal microscope systems (LSM 510) using a 63× 1.4 NA Plan Apochromat objective (Carl Zeiss, Inc.). Fluorescent chromatin was automatically tracked and focused during imaging using in-house developed macros (Rabut and Ellenberg, 2004). High-resolution imaging for Fig. 3 was performed with a 100× Plan Apochromat NA 1.4 objective (Carl Zeiss, Inc.).

Quantification and image analysis

Images were segmented on the chromatin channel in Image J (http://rsb.info.nih.gov/ij/) by successive application of a Gaussian and an anisotropic diffusion filter and thresholding of the filtered image with an in-house-developed macro. The segmentation was applied to the raw images of the IBB channel and the mean nuclear fluorescence intensities were quantified. For the assembly of most Nups, the same segmentation was used to quantify the mean intensity of the Nups on the chromatin region. During interphase, the soluble pools of both Nup50 and Nup153 localize to the nucleoplasm and a clear discrimination between nuclear rim association and nuclear import in later stages of mitosis could therefore not be achieved with the assay. However, the quantification on the nuclear rim region alone as compared with the complete chromatin region did not yield significantly different results for any of the two proteins, which suggests that the contribution of import to the measured kinetics is minor.

Manual rim segmentation was applied for all disassembly series to avoid folded regions of the NE. The apparent decrease in Nup133 fluorescence in the nuclear region after $t_{1/2}$(import) is caused by dilution of the signal during growth of the nuclear surface area in telophase upon chromatin decondensation. Mean intensities were background subtracted and normalized. Different time series were aligned according to the time of the half maximal IBB intensity ($t_{1/2}$[import]) in the nucleus (set to zero). Temporal alignment of assembly series along the metaphase–anaphase transition gave similar overall results but yielded consistently higher SDs and was therefore not pursued. The time point of first accumulation of signal over cytoplasmic background in the chromatin region was scored visually. For presentation purposes, images shown in Figs. 1, 2, 4, S1, and S2 were filtered with a Gaussian blur filter (Image J), kernel size 1. Error bars in all figures represent the SD.

Online supplemental material

Fig. S1 shows all individual disassembly/reassembly curves used to derive the mean kinetics shown in Fig. 5 (A and B). Fig. S2 shows representative image series for the assembly of Nup50, Nup98, Nup93, and Nup214 and mean assembly curves for all analyzed members of the Nup107–160 complex. Fig. S3 shows a representative image series for the disassembly of Nup133, Nup153, Nup93, and Nup214 and the localization of Nup50 on chromatin during mitosis. Videos 1 and 2 show representative assembly series forNup133 and Nup93, respectively. Videos 3 and 4 show disassembly series for POM121 and Nup98. Online supplemental material is available at http://www.jcb.org/cgi/content/full/jcb.200707026/DC1.

We would like to thank Katharina Ribbeck and Dirk Görlich for the IBB construct.

J. Ellenberg acknowledges funding by the Deutsche Forschungsgemeinschaft priority program SPP1175 (DFG EL 246/3-1). E. Dultz was supported by a fellowship from the European Molecular Biology Laboratory International PhD Program.

Submitted: 3 July 2007
Accepted: 5 February 2008

References

Beaudouin, J., D. Gerlich, N. Daigle, R. Eils, and J. Ellenberg. 2002. Nuclear envelope breakdown proceeds by microtubule-induced tearing of the lamina. *Cell.* 108:83–96.

Belgareh, N., G. Rabut, S.W. Bai, M. van Overbeek, J. Beaudouin, N. Daigle, O.V. Zatsepina, F. Pasteau, V. Labas, M. Fromont-Racine, et al. 2001. An evolutionarily conserved NPC subcomplex, which redistributes in part to kinetochores in mammalian cells. *J. Cell Biol.* 154:1147–1160.

Boehmer, T., J. Enninga, S. Dales, G. Blobel, and H. Zhong. 2003. Depletion of a single nucleoporin, Nup107, prevents the assembly of a subset of nucleoporins into the nuclear pore complex. *Proc. Natl. Acad. Sci. USA.* 100:981–985.

Burke, B., and J. Ellenberg. 2002. Remodelling the walls of the nucleus. *Nat. Rev. Mol. Cell Biol.* 3:487–497.

Cotter, L., T.D. Allen, E. Kiseleva, and M.W. Goldberg. 2007. Nuclear membrane disassembly and rupture. *J. Mol. Biol.* 369:683–695.

Daigle, N., J. Beaudouin, L. Hartnell, G. Imreh, E. Hallberg, J. Lippincott-Schwartz, and J. Ellenberg. 2001. Nuclear pore complexes form immobile networks and have a very low turnover in live mammalian cells. *J. Cell Biol.* 154:71–84.

D'Angelo, M.A., D.J. Anderson, E. Richard, and M.W. Hetzer. 2006. Nuclear pores form de novo from both sides of the nuclear envelope. *Science.* 312:440–443.

Ellenberg, J., E.D. Siggia, J.E. Moreira, C.L. Smith, J.F. Presley, H.J. Worman, and J. Lippincott-Schwartz. 1997. Nuclear membrane dynamics and reassembly in living cells: targeting of an inner nuclear membrane protein in interphase and mitosis. *J. Cell Biol.* 138:1193–1206.

Franz, C., R. Walczak, S. Yavuz, R. Santarella, M. Gentzel, P. Askjaer, V. Galy, M. Hetzer, I.W. Mattaj, and W. Antonin. 2007. MEL-28/ELYS is required for the recruitment of nucleoporins to chromatin and postmitotic nuclear pore complex assembly. *EMBO Rep.* 8:165–172.

Galy, V., P. Askjaer, C. Franz, C. Lopez-Iglesias, and I.W. Mattaj. 2006. MEL-28, a novel nuclear-envelope and kinetochore protein essential for zygotic nuclear-envelope assembly in *C. elegans*. *Curr. Biol.* 16:1748–1756.

Gerlich, D., J. Beaudouin, B. Kalbfuss, N. Daigle, R. Eils, and J. Ellenberg. 2003. Global chromosome positions are transmitted through mitosis in mammalian cells. *Cell.* 112:751–764.

Goldberg, M.W., C. Wiese, T.D. Allen, and K.L. Wilson. 1997. Dimples, pores, star-rings, and thin rings on growing nuclear envelopes: evidence for structural intermediates in nuclear pore complex assembly. *J. Cell Sci.* 110:409–420.

Gorlich, D., P. Henklein, R.A. Laskey, and E. Hartmann. 1996. A 41 amino acid motif in importin-alpha confers binding to importin-beta and hence transit into the nucleus. *EMBO J.* 15:1810–1817.

Harel, A., R.C. Chan, A. Lachish-Zalait, E. Zimmerman, M. Elbaum, and D.J. Forbes. 2003a. Importin beta negatively regulates nuclear membrane fusion and nuclear pore complex assembly. *Mol. Biol. Cell.* 14:4387–4396.

Harel, A., A.V. Orjalo, T. Vincent, A. Lachish-Zalait, S. Vasu, S. Shah, E. Zimmerman, M. Elbaum, and D.J. Forbes. 2003b. Removal of a single pore subcomplex results in vertebrate nuclei devoid of nuclear pores. *Mol. Cell.* 11:853–864.

Hase, M.E., and V.C. Cordes. 2003. Direct interaction with nup153 mediates binding of Tpr to the periphery of the nuclear pore complex. *Mol. Biol. Cell.* 14:1923–1940.

Hutten, S., and R.H. Kehlenbach. 2006. Nup214 is required for CRM1-dependent nuclear protein export in vivo. *Mol. Cell. Biol.* 26:6772–6785.

Kiseleva, E., S. Rutherford, L.M. Cotter, T.D. Allen, and M.W. Goldberg. 2001. Steps of nuclear pore complex disassembly and reassembly during mitosis in early *Drosophila* embryos. *J. Cell Sci.* 114:3607–3618.

Lenart, P., G. Rabut, N. Daigle, A.R. Hand, M. Terasaki, and J. Ellenberg. 2003. Nuclear envelope breakdown in starfish oocytes proceeds by partial NPC disassembly followed by a rapidly spreading fenestration of nuclear membranes. *J. Cell Biol.* 160:1055–1068.

Loiodice, I., A. Alves, G. Rabut, M. Van Overbeek, J. Ellenberg, J.B. Sibarita, and V. Doye. 2004. The entire Nup107-160 complex, including three new members, is targeted as one entity to kinetochores in mitosis. *Mol. Biol. Cell.* 15:3333–3344.

Mansfeld, J., S. Guttinger, L.A. Hawryluk-Gara, N. Pante, M. Mall, V. Galy, U. Haselmann, P. Muhlhausser, R.W. Wozniak, I.W. Mattaj, et al. 2006. The conserved transmembrane nucleoporin NDC1 is required for nuclear pore complex assembly in vertebrate cells. *Mol. Cell.* 22:93–103.

Matsuoka, Y., M. Takagi, T. Ban, M. Miyazaki, T. Yamamoto, Y. Kondo, and Y. Yoneda. 1999. Identification and characterization of nuclear pore

subcomplexes in mitotic extract of human somatic cells. *Biochem. Biophys. Res. Commun.* 254:417–423.

Osmani, A.H., J. Davies, H.L. Liu, and S.A. Osmani. 2006. Systematic deletion and mitotic localization of the nuclear pore complex proteins of *Aspergillus nidulans*. *Mol. Biol. Cell.* 17:4946–4961.

Rabut, G., and J. Ellenberg. 2004. Automatic real-time three-dimensional cell tracking by fluorescence microscopy. *J. Microsc.* 216:131–137.

Rabut, G., V. Doye, and J. Ellenberg. 2004a. Mapping the dynamic organization of the nuclear pore complex inside single living cells. *Nat. Cell Biol.* 6:1114–1121.

Rabut, G., P. Lenart, and J. Ellenberg. 2004b. Dynamics of nuclear pore complex organization through the cell cycle. *Curr. Opin. Cell Biol.* 16:314–321.

Rasala, B.A., A.V. Orjalo, Z. Shen, S. Briggs, and D.J. Forbes. 2006. ELYS is a dual nucleoporin/kinetochore protein required for nuclear pore assembly and proper cell division. *Proc. Natl. Acad. Sci. USA.* 103:17801–17806.

Ribbeck, K., and D. Gorlich. 2002. The permeability barrier of nuclear pore complexes appears to operate via hydrophobic exclusion. *EMBO J.* 21:2664–2671.

Schmid, M., G. Arib, C. Laemmli, J. Nishikawa, T. Durussel, and U.K. Laemmli. 2006. Nup-PI: the nucleopore-promoter interaction of genes in yeast. *Mol. Cell.* 21:379–391.

Shaner, N.C., R.E. Campbell, P.A. Steinbach, B.N. Giepmans, A.E. Palmer, and R.Y. Tsien. 2004. Improved monomeric red, orange and yellow fluorescent proteins derived from *Discosoma* sp. red fluorescent protein. *Nat. Biotechnol.* 22:1567–1572.

Stavru, F., B.B. Hulsmann, A. Spang, E. Hartmann, V.C. Cordes, and D. Gorlich. 2006. NDC1: a crucial membrane-integral nucleoporin of metazoan nuclear pore complexes. *J. Cell Biol.* 173:509–519.

Suntharalingam, M., and S.R. Wente. 2003. Peering through the pore: nuclear pore complex structure, assembly, and function. *Dev. Cell.* 4:775–789.

Walther, T.C., H.S. Pickersgill, V.C. Cordes, M.W. Goldberg, T.D. Allen, I.W. Mattaj, and M. Fornerod. 2002. The cytoplasmic filaments of the nuclear pore complex are dispensable for selective nuclear protein import. *J. Cell Biol.* 158:63–77.

Walther, T.C., A. Alves, H. Pickersgill, I. Loiodice, M. Hetzer, V. Galy, B.B. Hulsmann, T. Kocher, M. Wilm, T. Allen, et al. 2003a. The conserved Nup107-160 complex is critical for nuclear pore complex assembly. *Cell.* 113:195–206.

Walther, T.C., P. Askjaer, M. Gentzel, A. Habermann, G. Griffiths, M. Wilm, I.W. Mattaj, and M. Hetzer. 2003b. RanGTP mediates nuclear pore complex assembly. *Nature.* 424:689–694.

Wiese, C., M.W. Goldberg, T.D. Allen, and K.L. Wilson. 1997. Nuclear envelope assembly in *Xenopus* extracts visualized by scanning EM reveals a transport-dependent 'envelope smoothing' event. *J. Cell Sci.* 110:1489–1502.

Wozniak, R., and P.R. Clarke. 2003. Nuclear pores: sowing the seeds of assembly on the chromatin landscape. *Curr. Biol.* 13:R970–R972.

Yang, L., T. Guan, and L. Gerace. 1997. Integral membrane proteins of the nuclear envelope are dispersed throughout the endoplasmic reticulum during mitosis. *J. Cell Biol.* 137:1199–1210.

Ye, Q., and H.J. Worman. 1994. Primary structure analysis and lamin B and DNA binding of human LBR, an integral protein of the nuclear envelope inner membrane. *J. Biol. Chem.* 269:11306–11311.